Desalination and Water Treatment
www.deswater.com

doi:10.5004/dwt.2019.24006

153 (2019) 349–356
June

Effective and selective removal of cationic dye from aqueous solution using rosin derivative modified wheat straw

Lei Hu[a], Limin Zang[a,*], Qifan Liu[b], Jianhui Qiu[b], Chao Yang[a,*], Xu Xu[a], Jun Yang[a], Xuan Qiao[a]

[a]*Key Laboratory of New Processing Technology for Nonferrous Metal and Materials (Ministry of Education), and College of Materials Science and Engineering, Guilin University of Technology, Guilin 541004, China, Tel. +86 773 5896672, email: hlpolymer010@gmail.com (L. Hu), 2016034@glut.edu.cn (L. Zang), 2011012@glut.edu.cn (C. Yang), xuxu8485@163.com (X. Xu), yjun013@gmail.com (J. Yang), qiaoxuan150103@gmail.com (X. Qiao)*
[b]*Department of Machine Intelligence and Systems Engineering, Faculty of Systems Science and Technology, Akita Prefectural University, Yurihonjo 015-0055, Japan, Tel. +81 184 272134, email: liuqifan0108@gmail.com (Q. Liu), qiu@akita-emails:pu.ac.jp (J. Qiu)*

Received 8 July 2018; Accepted 19 February 2019

ABSTRACT

This study developed an effective, low-cost and renewable bioadsorbent to remove dyes from wastewater. Wheat straw, an agricultural by-product with abundant resource, was modified with rosin derivative (maleated rosin) and applied as a biosorbent to improve adsorption capacity and selectivity for cationic dyes [(e.g., methylene blue (MB)]. The effects of pH, contact time, temperature and regeneration on adsorption were investigated and discussed. The MB adsorption capacity of the rosin derivative modified wheat straw was 113.34 mg/g, and low temperature and alkaline environment was in favor of the MB adsorption onto the bioadsorbent. The kinetic data was fitted well by pseudo-second-order kinetic model, and equilibrium adsorption isotherm data was fitted well by Freundlich and Temkin isotherm models. In addition, the bioadsorbent could be regenerated in acid condition and reused for several cycles. All the results indicate that the rosin derivative modified wheat straw is a promising bioadsorbent for wastewater treatment.

Keywords: Wheat straw; Rosin; Bioadsorbent; Selective adsorption; Regeneration

1. Introduction

Massive amounts of synthetic organic dyes are annually consumed by various sectors including textile, papermaking, plastic, leather and cosmetic industries, especially in developing countries. The wastewater results in vast serious harmful effects on environmental issues and even threat to the human health due to their carcinogenic and toxic characteristics if these dyes directly pour into rivers and lakes without treatment [1]. Many techniques have been employed to eliminate dyes from wastewater which involve adsorption [2], flocculation [3], oxidation [4], and electrolysis [5]. Among them, adsorption is considered to be superior by virtue of the simple process, high efficiency and good removal of various dyes [6–8]. Although many adsorbents have been developed for removing dyes from aqueous solution, such as activated carbon, natural clays and synthetic resins, the high-cost in production and regeneration of adsorbents will limit their application in large scale [9,10]. Therefore, many researchers have made great efforts in developing new adsorbents which have high cost-efficiency and adsorption capacity to reduce the overall cost of the wastewater disposal.

Developing agricultural by-products or wastes for effective, low-cost, biodegradable and renewable bioadsorbents have attracted more and more research attention [11–13]. To date, a variety of low-cost agricultural by-products including corn straw, peanut hull, rice husk and so on have

*Corresponding author.

been prepared as the bioadsorbents for dyes adsorption by convenient methods [14–16]. Wheat is widely grown in many regions and countries, which means a vast amount of wheat straw is produced annually. However, the natural wheat straw (NWS) without modification is not effective to remove ionic dyes due to the lack of functional groups [17]. Therefore, it is possible improve ionic dyes adsorption capacity effectively by the introduction of functional groups onto the surface of NWS.

As an abundant renewable resource, rosin is a kind of solid resin and consists of various resin acids, especially abietic acid, which is obtained from pine trees and some other-conifers. Rosin and its derivatives also exhibit wide-ranging applications in food, chemical and pharmaceuticals [18,19]. Compared with traditional modifiers such as glycidol and synthetic surfactants, rosin is a non-toxic natural material and low-cost which attracts our attention to use it to modify NWS to improve ionic dyes adsorption capacity. The objectives of this work include: (1) modification of NWS by rosin derivative and using it as a bioadsorbent for removing cationic dyes from aqueous solution; (2) studying the effects of pH, temperature, contact time, initial dye concentration and regeneration on adsorption; (3) analysis of the adsorption mechanism of MB adsorption onto MRS according to adsorption kinetics and isotherms; (4) investigation of mechanism of the MRS for selective removing of cationic dyes.

2. Materials and methods

2.1. Materials

Methylene blue (MB), acid fuchsin (AF), maleic anhydride and glacial acetic acid were bought from Aladdin Chemistry Co. Ltd. (Shanghai, China). Rosin was obtained from Xingsonglinhua Chemical Co., Ltd. (Guilin, China). The natural wheat straw (NWS, 106~300 μm) in this work was collected from Gansu province, China. Hydrochloric acid (HCl) and sodium hydroxide (NaOH) were purchased from Xilong Chemical Co., Ltd. (Guangdong, China). Deionized water was used as solvent in the experiments.

2.2. Preparation of the bioadsorbent

2.2.1. Synthesis of maleated rosin

Maleated rosin was prepared from rosin and maleic anhydride according to the previous report. The synthetic process was basically performed as follows: 50 g Rosin was firstly melted at 140°C. Then 12 g malic anhydrid was added and the mixture was heated to 170°C under mechanical stirring for 2 h. Subsequently, 100 mL glacial acetic acid was added into the reaction mixture after cooling to room temperature. The reaction temperature was raised again to obtain the homogeneous solution under stirring, and then cooled to obtain white powder. The resulting powder was dried at 60°C after filtering and washing for several times with deionized water and ethanol.

2.2.2. Preparation of modified wheat straw (MRS)

The wheat straw was modified with the maleated rosin as a bioadsorbent and the preparation process is shown in Fig. 1. Briefly, 17.5g dry NWS and 24.5 g maleated rosin were added into 175 mL xylene. The mixture was heated to 130°C for 5 h under mechanical stirring. The resulting precipitate was filtered and washed with ethanol for several times. The final product was dried at 60°C in an oven.

2.3. Adsorption studies

A stock dye solution was prepared in advance by dissolving 1 g MB in 1 L distilled water. MB solutions with different initial concentrations (80–180 mg/L) were obtained from the dilution of the stock solution in accurate ratio. The pH of MB solution was adjusted by 0.1 mol/L HCl or 0.1 mol/L NaOH solution from 5 to 10. For adsorption experiment, 0.05 g bioadsorbent (MRS) and 50 mL MB solution was mixed under magnetic stirring. When reaching the adsorption equilibrium, the bioadsorbent was separated by MCE syringe filter (pore size: 0.22 μm). Then the supernatant solution was taken out and the final concentration of MB was measured by a UV-vis spectrophotometer

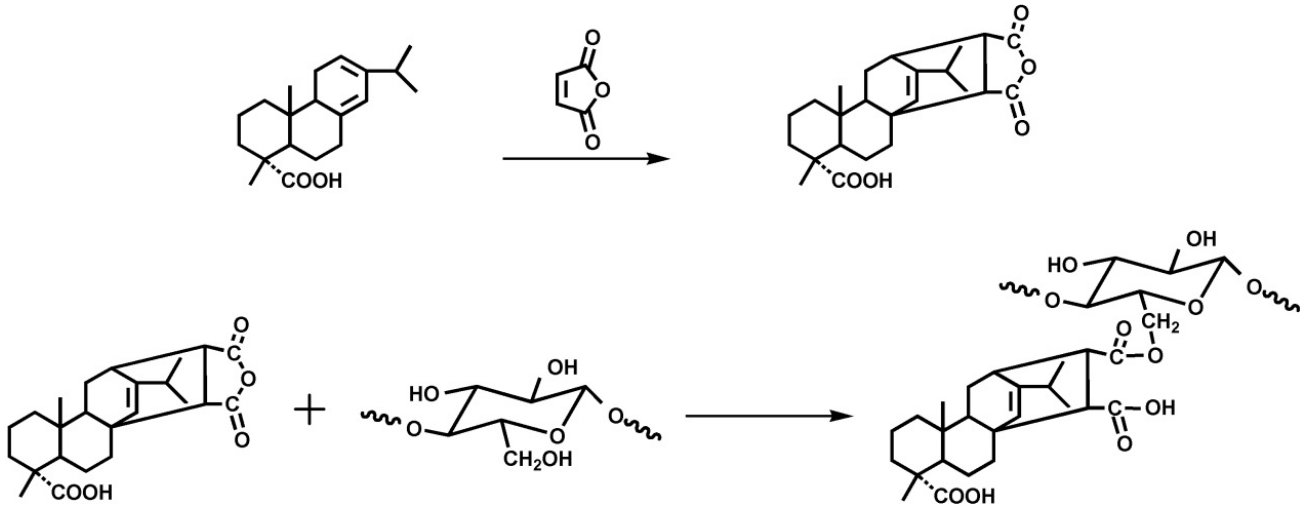

Fig. 1. Synthesis of MRS (cellulose as example).

(λ_{max} = 664 nm). The kinetics experiment required different contact times (10–1440 min) at invariant temperature and pH. For the isothermal equilibrium study, the batch adsorption experiments were conducted in a water-bath at different initial concentrations (80–180 mg/L) at 25°C.

The adsorption capacity was obtained by the following equation:

$$q_e = \frac{(C_0 - C_e)V}{m} \quad (1)$$

where q_e (mg/g) is the adsorption capacity at equilibrium; c_0 is the initial concentration of MB solution; c_e is the equilibrium concentration of MB solution; V (L) is the volume of MB solution; m (g) is the mass of bioadsorbent.

2.4. Characterization

The Fourier transform infrared spectroscopy (FTIR) measurements (Thermo Nexus 470 FTIR spectrometer) were carried out with the KBr pellet method. Thermogravimetric results were obtained with a thermogravimetric analyzer (TA Instrument Q500) at a heating rate of 10°C/min from 25 to 700°C under nitrogen atmosphere. UV-vis absorption spectra were recorded on a UV-vis spectrophotometer (752N, INESA Analytical Instrument Co., Ltd.). The pH values of solutions were measured with a pH meter (PHS-25, Shanghai Precision & Scientific Instrument Co., Ltd).

3. Results and discussion

3.1. Characterization of the bioadsorbents

FTIR spectra shown in Fig. 2 was used to confirm the functional groups of NWS and MRS. The characteristic peaks around 3420, 2923 and 1100 cm^{-1} appeared in both NWS and MRS, which were attributed to the stretching vibrations of hydroxyl groups, C-H in methylene groups and C-OH groups, respectively [20]. The results recorded with the existence of abundant polysaccharide substance such as cellulose and lignin in NWS [21]. Compared with NWS, the stretching vibration adsorption peaks of MRS at 2920 cm^{-1} ($-CH_2$) and 1635 cm^{-1} (C=O) were enhanced, which indicated that MRS had more ester groups than NWS. The results confirmed that maleated rosin was successfully introduced into wheat straw after modification.

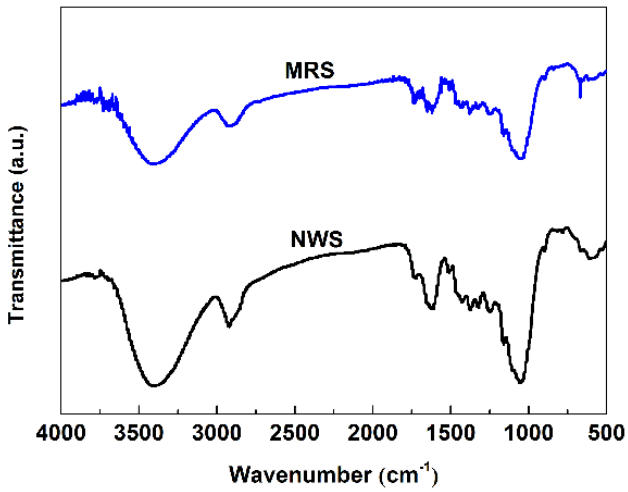

Fig. 2. FTIR spectra of MRS and NWS.

Thermogravimetric analysis (TGA) of MRS and NWS were conducted to comprehend the weight loss of the both bioadsorbents. Fig. 3 shows that MRS and NWS were pyrolysed below 550°C and 25% of residues were remained. A small mass loss of 9% below 100°C was seen due to the loss of moisture. DTG curves demonstrated the maximum decomposition temperature of MRS and NWS was at 320°C because most substances such as the cellulose were decomposed [22,23]. The extra small peak of MRS appeared at 210°C while NWS did not have. The reason might be the decomposition of maleated rosin in MRS. The results also proved the successful modification of wheat straw with maleated rosin.

3.2. Effect of pH on adsorption

The pH of dye solution is a key factor in the adsorption process, particularly important for the adsorption capacity. It influences not only the surface charge and dissociation of functional groups on the active sites of the adsorbent, but also the solution dye chemistry. Fig. 4 shows the MB adsorption capacities of MRS and NWS at pH from 5 to 10. The minimum MB adsorption capacities were at pH 5–6 because of the protonation and electrostatic repulsion between the bioadsorbents and MB. When the pH increased from 6 to 9, deprotonating and electrostatic attraction between bioadsorbents and MB occurred, leading to higher MB adsorption capacities. MRS exhibited more superior dye adsorption capacity than NWS owing to the successful modification. Specifically, more functional groups (–COOH) were introduced onto the surface of wheat straw by modification with maleated rosin, and they were deprotonated and became $–COO^-$ in alkaline environment which was conducive to enhancing the interaction between MRS and MB. It's worth mentioning that our MRS also showed better performance in dye adsorption capacity than some reported modified natural materials [24–30] as well as lower cost than active carbon [31], indicating our MRS is a promising bioadsorbent for cationic dyes adsorption.

3.3. Effect of contact time on adsorption and kinetic analysis

Fig. 5 shows the effect of contact time on MB adsorption capacity of MRS at different MB initial concentrations at 25°C. The adsorption process was divided into three stages: (1) a rapid initial stage where adsorption rate was fast; (2) a slow second stage where adsorption rate became lower; (3) the slowest equilibrium adsorption stage. The equilibrium time and adsorption capacity increased as the MB initial concentration increased. The equilibrium time of MB onto MRS was about 600, 1200 and 1440 min, and the adsorption quantities were up to 87.86, 102.39 and 113.34 mg/g when the MB initial concentration was 100, 120 and 140 mg/g, respectively.

In order to explain kinetic mechanisms of the adsorption process, several kinetic models were applied to analyze the

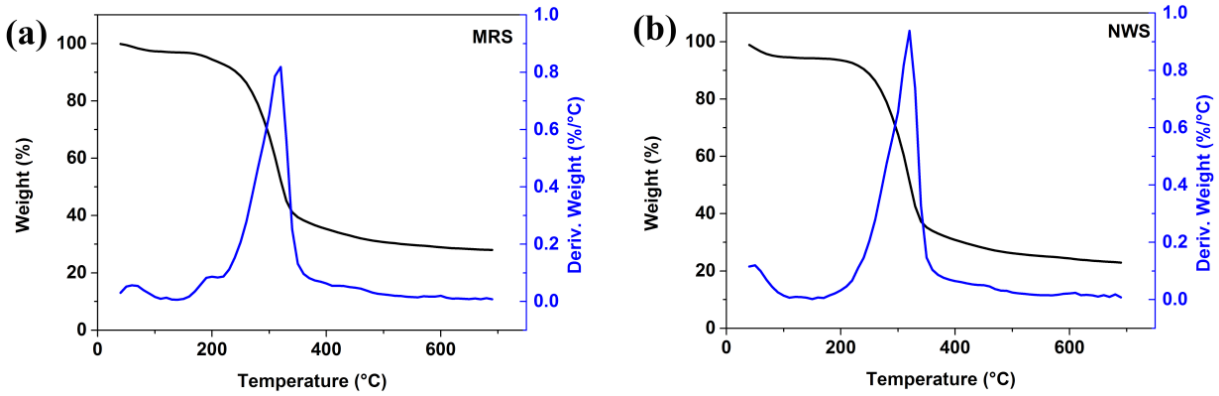

Fig. 3. The TGA (black) and DTG (blue) curves of MRS (a) and NWS(b).

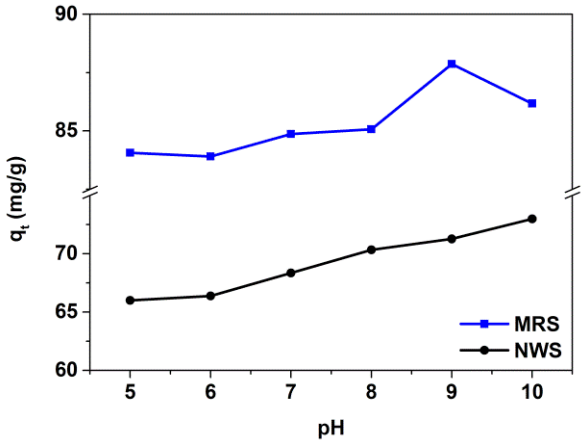

Fig. 4. The effect of pH on the MB adsorption capacities of MRS and NWS (c_0 = 100 mg/L, t = 1440min, T = 25°C).

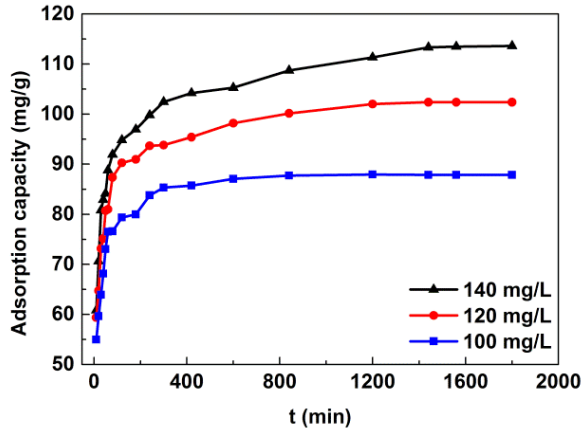

Fig. 5. The effect of contact time on MB adsorption capacity of MRS.

experimental data. The pseudo-first-order model and pseudo-second-order kinetic model are expressed as follows:

Pseudo-first-order kinetic model: $\ln(q_e - q_t) = \ln q_e - k_1 t$ (2)

Pseudo-second-order kinetic model: $t/q_t = t/q_e + 1/k_2 q_e^2$ (3)

where q_t (mg/g) is the adsorption capacity at time t; k_1 (1/min) and k_2 (g/mg×min) is the pseudo-first-order kinetic rate constant and pseudo-second-order kinetic model rate constant, respectively.

Table 1 shows the relevant parameters of each kinetic model. As we know, the regression correlation coefficient (R^2) is significant for the linear analysis, of which the R^2 is approximate to 1, the degree of coincidence would be better. The pseudo-first-order model was not so suited the adsorption process from Fig. 6a and Table 1. As shown in Fig. 6b and Table 1, all the values of R^2 were higher than 0.99 and the calculated values of adsorption capacity ($q_{e,cal}$) for pseudo-second-order kinetic model were closer to the experimental values of adsorption capacity ($q_{e,exp}$), which indicated MB adsorption onto MRS obeyed pseudo-second-order kinetic model well. The adsorption process was the rate-determining step including electron sharing or exchange between MRS and MB ions [32].

The dyes transferred from solution to the surface of adsorbent particles via a few steps, involving external surface diffusion and intraparticle diffusion. To further investigate the adsorption mechanism, the kinetic data was fitted by intraparticle diffusion model according to the following equation:

Intraparticle diffusion model: $q_t = k_p t^{1/2} + C$ (4)

where k_p (mg/g·min$^{1/2}$) is the intraparticle diffusion rate constant; C is the intercept of this model.

Plots of intraparticle diffusion model for MB adsorption onto MRS at different MB concentrations are shown in Fig. 7 and the parameters are given in Table 2. The multi-linear plots proved that other adsorption steps in the whole adsorption process existed. The linear curves of MRS didn't pass through the origin. The values of C were nonzero, meaning the diffusion process wasn't the only rate-limiting step. In other word, larger value of C means surface adsorption has greater effect on adsorption process [33]. Therefore, the adsorption process may be divided into three steps, including surface adsorption, intraparticle diffusion and equilibrium stage [34]. Among these steps, the first step was surface adsorption

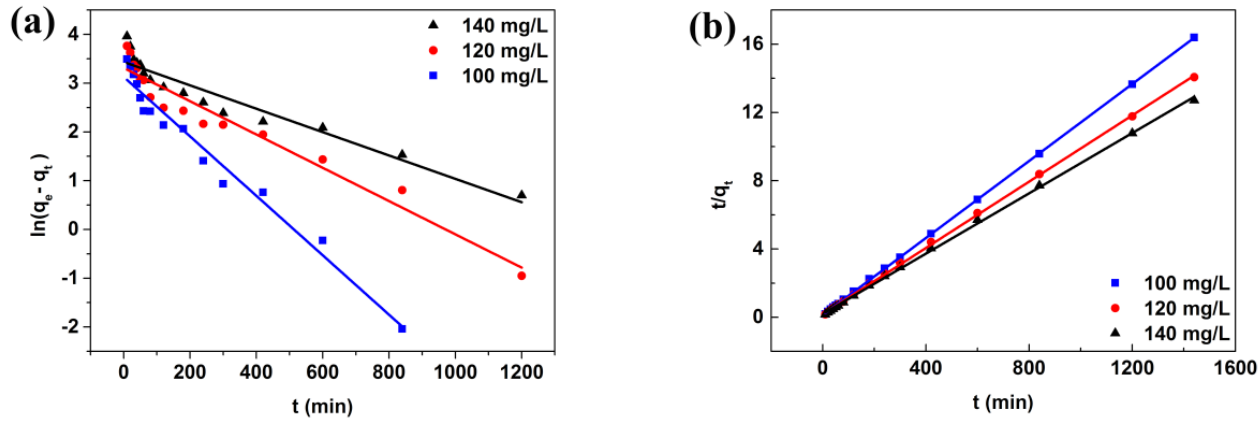

Fig. 6. Plots of pseudo-first-order (a) and pseudo-second-order (b) for MB adsorption onto MRS at different MB concentrations.

Table 1
Parameters of kinetic models for MB absorption onto MRS

MB (mg/L)	$q_{e,exp}$ (mg/g)	Pseudo-first-order kinetic model			Pseudo-second-order kinetic mode		
		k_1 (1/min)	$q_{e,cal}$ (mg/g)	R^2	k_2 (g/mg·min)	$q_{e,cal}$ (mg/g)	R^2
100	87.86	0.006	22.85	0.9676	0.0009	88.65	0.9999
120	102.39	0.003	27.47	0.9443	0.0005	102.99	0.9996
140	113.34	0.002	31.05	0.9142	0.0004	113.25	0.9992

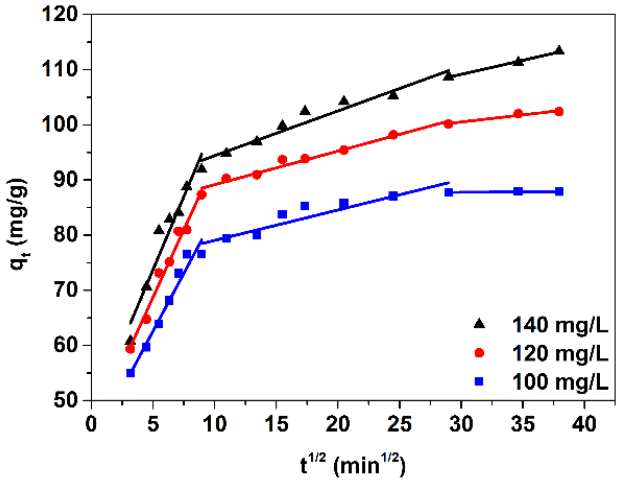

Fig. 7. Plots of intraparticle diffusion model for MB adsorption onto MRS at different MB concentrations.

which was controlled by external mass transfer because of the electrostatic attraction. The second step was gradually controlled by the intraparticle diffusion and the last stage was equilibrium portion.

3.4. Adsorption isotherms

Fig. 8 shows the equilibrium isotherms of MB adsorption onto MRS at 25°C. Obviously, the value of q_e became higher as the c_e increased. Three adsorption isotherm models were applied to analyze the adsorption equilibrium data. Generally, Langmuir isotherm model is used to describe the monolayer adsorption process on the homogeneous surface without interaction. Freundlich isotherm model is a semi-empirical equation, which describes the heterogeneous surface adsorption. Temkin isotherm model describes that the adsorption heat linearly falls down with the increasing adsorption capacity [35]. The three models are presented as follows:

Langmuir isotherm model: $$q_e = \frac{q_m K_L C_e}{1 + K_L C_e} \quad (5)$$

Freundlich isotherm model: $$q_e = K_F C_e^{1/n} \quad (6)$$

Temkin isotherm model: $$q_e = A + B \ln C_e \quad (7)$$

where q_m (mg/g) is the maximum adsorption capacity; C_e is the equilibrium concentration of dye; K_L (L/mg) and K_F (mg/g) is the Langmuir adsorption constant and Freundlich adsorption constant, respectively; $1/n$ is a constant related to the adsorption intensity; A and B are the Temkin constants.

Relevant parameters of the three isotherm models are listed in Table 3. The values of R^2 for Freundlich and Temkin isotherm models were higher than that of Langmuir isotherm model, indicating Freundlich and Temkin isotherm models fitted the adsorption equilibrium data better. Therefore, the adsorption process of MB adsorption onto MRS was complex and included several mechanisms. In addition, the value of $1/n$ was 0.28, meaning that the MB adsorption onto MRS was favorable.

Table 2
Parameters of intraparticle diffusion model for MB absorption onto MRS

MB (mg/L)	Intraparticle diffusion model								
	k_{p1} (mg/g·min$^{1/2}$)	C_1 (mg/g)	R^2	k_{p2} (mg/g·min$^{1/2}$)	C_2 (mg/g)	R^2	k_{p3} (mg/g·min$^{1/2}$)	C_3 (mg/g)	R^2
100	4.187	41.69	0.9539	0.551	73.54	0.8349	0.017	87.28	1
120	4.892	44.30	0.9753	0.608	83.08	0.9674	0.258	92.78	1
140	5.301	47.28	0.9257	0.812	86.30	0.9391	0.510	93.85	1

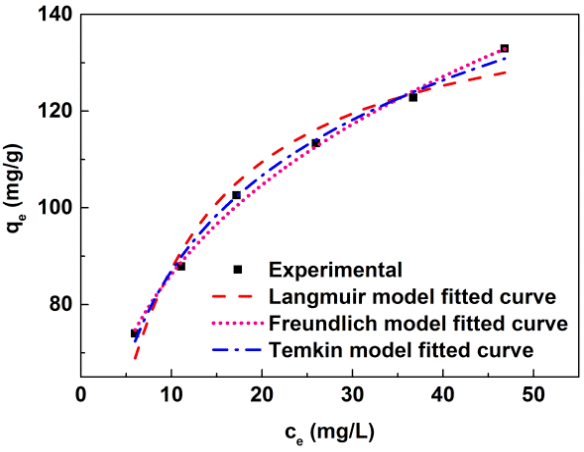

Fig. 8. Adsorption isotherms of MB adsorption onto MRS.

3.5. Thermodynamic parameters

Thermodynamic parameters of the Gibb's free energy change (ΔG^0), enthalpy change (ΔH^0), entropy change (ΔS^0) and distribution coefficient (K_c) for MB adsorption onto MRS were determined as follows [36]:

$$K_c = C_{ad,e} / C_e \quad (8)$$

$$\Delta G^0 = -RTlnK_c \quad (9)$$

$$\Delta G^0 = \Delta H^0 - T\Delta S^0 \quad (10)$$

where $C_{ad,e}$ (mg/L) is the MB concentration on the adsorbent at equilibrium; R (8.314 J/mol·K) is the universal gas constant; T (K) is the experimental temperature.

These determined thermodynamic parameters are shown in Table 4. The negative values of ΔG^0 at three temperatures indicated that the adsorption process was feasible and spontaneous. The values of ΔG^0 increased with the increasing temperature, which demonstrated that lower temperature was in favor of the MB adsorption onto MRS. The negative value of ΔH^0 represented the exothermic nature of adsorption process. The negative value of ΔS^0 explained a decrease in randomness at the solid/solution interface.

3.6. Selective adsorption

It is significant to separate specific dye from a mixed solution in practical applications. In this work, a number of –COOH groups were presented on the surface of MRS, meaning that MRS would have stronger interaction with cationic dyes t than anionic dyes. Therefore, it is possible to use MRS as a selective bioadsorbent for cationic dyes from the mixture of dyes. In order to identify this opinion, the mixture of MB (cationic dye) and AF (anionic dye) was used as the experimental sample to evaluate the selective adsorption performance of MRS. As shown in Fig. 9, the color of the MB/AF mixture was purple, and two main peaks appeared at 546 nm (AF) and 664 nm (MB) in the UV-vis spectrum. After adsorption by MRS, the solution was red and only one peak appeared at 546 nm in the UV-vis spectrum, indicating MRS exhibited high selective adsorption for cationic dyes.

3.7. Regeneration study

To reduce the cost of in practical applications, the adsorbent should be easily regenerated and the adsorbate should be efficiently recovered. Thus desorption capability is also important to evaluate the performance of MRS. According to the previous reports, the cationic dye solution can be desorbed well in an acid condition, which indicates that the adsorption process is controlled by ion exchange chiefly [30]. In this work, 0.1 mol/L HCl solution was used to regenerate the MRS for five cycles, and the results are given in Fig. 10. For the first three cycles, MRS showed great regeneration property and the removal efficiency was higher than 90%. For the fifth cycle, the removal efficiency decreased to ~70% because the chemisorption of dye molecules may result in some loss of adsorption capacities and the complete regeneration of dye-loaded MRS is impossible.

4. Conclusion

The maleated rosin modified wheat straw (MRS) was prepared and characterized in this work. This bioadsorbent exhibited excellent adsorption capacity and selectivity for cationic dye from aqueous solution owing to the increased functional groups on the surface of MRS. Moreover, the MRS also showed good regeneration property and removal efficiency. The adsorption process may include three steps: surface adsorption, intra particle diffusion and equilibrium stage. The process of MB adsorption onto MRS was spontaneous and performed better at low temperature and alkaline environment. The results demonstrate that the MRS is low-cost, efficient and environmental-friendly which can be used as a promising bioadsorbent for cationic dyes adsorption from wastewater.

Table 3
Parameters of adsorption isotherms for MB absorption onto MRS

Langmuir isotherm model			Freundlich isotherm model			Temkin isotherm model		
q_m (mg/g)	K_L (L/mg)	R^2	K_F (mg/g)	1/n	R^2	A	B	R^2
146.40	0.1481	0.9607	45.25	0.28	0.9956	21.38	28.47	0.9933

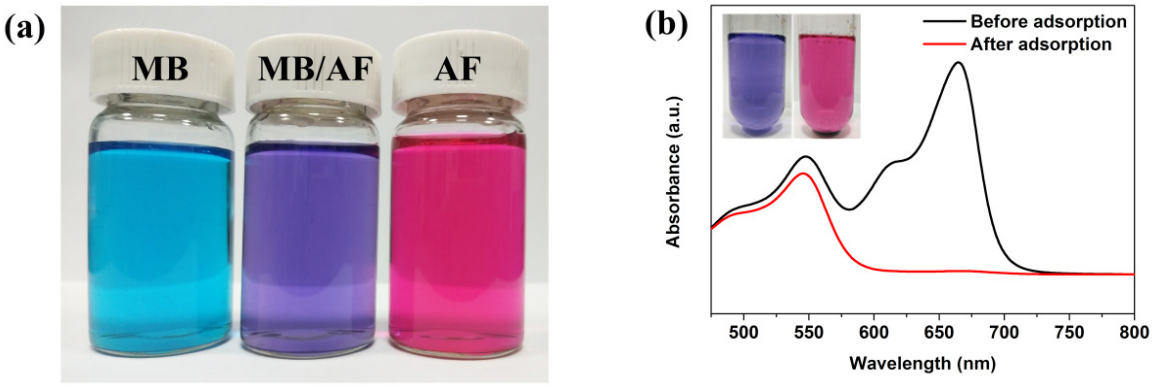

Fig. 9. Digital images of MB, MB/AF mixture and AF (a); UV-vis spectra of the MB/AF mixture before and after adsorption by MRS (b).

Table 4
Thermodynamic parameters of MB absorption onto MRS

T (K)	298	308	318
ΔG^0 (kJ/mol)	–4.47	–4.02	–3.57
ΔH^0 (kJ/mol)	–17.91		
ΔS^0 (kJ/mol·K)	–0.045		

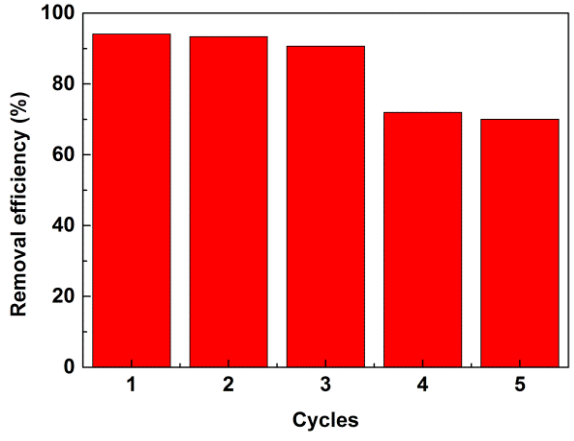

Fig. 10. Regeneration property of MRS.

Acknowledgements

The work was supported by the Guangxi Natural Science Foundation (No. 2017GXNSFBA198085), Scientific Research Foundation of Guilin University of Technology (No. GUTQDJJ2017002) and Project of Department of Science and Technology of Guilin (No. 2016012005).

References

[1] E. Daneshvar, A. Vazirzadeh, A. Niazi, M. Kousha, M. Naushad, A. Bhatnagar, Desorption of Methylene blue dye from brown macroalga: Effects of operating parameters, isotherm study and kinetic modeling, J. Clean Prod., 152 (2017) 443–453.
[2] H. Ma, S. Pu, Y. Hou, R. Zhu, A. Zinchenko, W. Chu, A highly efficient magnetic chitosan "fluid" adsorbent with a high capacity and fast adsorption kinetics for dyeing wastewater purification, Chem. Eng. J., 345 (2018) 556–565.
[3] M.J. Puchana-Rosero, E.C. Lima, B. Mella, D. Costa, E. Poll, M. Gutterres, A coagulation-flocculation process combined with adsorption using activated carbon obtained from sludge for dye removal from tannery wastewater, J. Chil. Chem. Soc., 63 (2018) 3867–3874.
[4] X. Li, J.-L. Shi, H. Hao, X. Lang, Visible light-induced selective oxidation of alcohols with air by dye-sensitized TiO_2 photocatalysis, Appl. Catal., B, 232 (2018) 260–267.
[5] Y. Han, H. Li, M. Liu, Y. Sang, C. Liang, J. Chen, Purification treatment of dyes wastewater with a novel micro-electrolysis reactor, Sep. Purif. Technol., 170 (2016) 241–247.
[6] F. Xiao, J. Cheng, X. Fan, C. Yang, Y. Hu, Adsorptive removal of the hazardous anionic dye Congo red and mechanistic study of ZIF-8, Desal. Water Treat., 101 (2018) 291–300.
[7] Q. Yang, Y. Wang, J. Wang, F. Liu, N. Hu, H. Pei, W. Yang, Z. Li, Y. Suo, J. Wang, High effective adsorption/removal of illegal food dyes from contaminated aqueous solution by Zr-MOFs (UiO-67), Food Chem., 254 (2018) 241–248.
[8] Y. Guan, W. Cao, H. Guan, X. Lei, X. Wang, Y. Tu, A. Marchetti, X. Kong, A novel polyalcohol-coated hydroxyapatite for the fast adsorption of organic dyes, Colloids Surf., A, 548 (2018) 85–91.
[9] M.T. Yagub, T.K. Sen, S. Afroze, H.M. Ang, Dye and its removal from aqueous solution by adsorption: A review, Adv. Colloid Interface Sci., 209 (2014) 172–184.
[10] A. Kausar, M. Iqbal, A. Javed, K. Aftab, Z.-i.-H. Nazli, H.N. Bhatti, S. Nourend, Dyes adsorption using clay and modified clay: A review, J. Mol. Liq., 256 (2018) 395–407.
[11] C. Molina-Ramirez, C. Castro, R. Zuluaga, P. Ganan, Physical characterization of bacterial cellulose produced by komagataeibacter medellinensis using food supply chain waste and agricultural by-products as alternative low-cost feed stocks, J. Polym. Environ., 26 (2018) 830–837.

[12] A.T. Hoang, X.L. Bui, X.D. Pham, A novel investigation of oil and heavy metal adsorption capacity from as-fabricated adsorbent based on agricultural by-product and porous polymer, Energy Sources, Part A, 40 (2018) 929–939.
[13] K. Schaldach, V. Herdegen, H.-W. Schroder, J.-U. Repke, Activation and forming for improved properties of adsorbent materials from agricultural by-products, Chem. Ing. Tech., 89 (2017) 1669–1678.
[14] H. Ge, C. Wang, S. Liu, Z. Huang, Synthesis of citric acid functionalized magnetic graphene oxide coated corn straw for methylene blue adsorption, Bioresour. Technol., 221 (2016) 419–429.
[15] N. Tahir, H.N. Bhatti, M. Iqbal, S. Noreen, Biopolymers composites with peanut hull waste biomass and application for Crystal Violet adsorption, Int. J. Biol. Macromol., 94 (2017) 210–220.
[16] M. Shabandokht, E. Binaeian, H.-A. Tayebi, Adsorption of food dye acid red 18 onto polyaniline-modified rice husk composite: isotherm and kinetic analysis, Desal. Water Treat., 57 (2016) 27638–27650.
[17] H. You, J. Chen, C. Yang, L. Xu, Selective removal of cationic dye from aqueous solution by low-cost adsorbent using phytic acid modified wheat straw, Colloids Surf., A, 509 (2016) 91–98.
[18] X. Li, M. Li, J. Li, F. Lei, X. Su, M. Liu, P. Li, X. Tan, Synthesis and characterization of molecularly imprinted polymers with modified rosin as a cross-linker and selective SPE-HPLC detection of basic orange II in foods, Anal. Methods, 6 (2014) 6397–6406.
[19] P.M. Satturwar, S.V. Fulzele, J. Panyam, P.M. Mandaogade, D.R. Mundhada, B.B. Gogte, V. Labhasetwar, A.K. Dorle, Evaluation of new rosin derivatives for pharmaceutical coating, Int. J. Pharm., 270 (2004) 27–36.
[20] X. Han, W. Wang, X. Ma, Adsorption characteristics of methylene blue onto low cost biomass material lotus leaf, Chem. Eng. J., 171 (2011) 1–8.
[21] B.C. Oei, S. Ibrahim, S. Wang, H.M. Ang, Surfactant modified barley straw for removal of acid and reactive dyes from aqueous solution, Bioresour. Technol., 100 (2009) 4292–4295.
[22] K.K. Krishnani, X. Meng, C. Christodoulatos, V.M. Boddu, Biosorption mechanism of nine different heavy metals onto biomatrix from rice husk, J. Hazard. Mater., 153 (2008) 1222–1234.
[23] V. Dhanapal, K. Subramanian, Modified chitosan for the collection of reactive blue 4, arsenic and mercury from aqueous media, Carbohydr. Polym., 117 (2015) 123–132.
[24] S.K. Parida, S. Dash, S. Patel, dB.K. Mishra, Adsorption of organic molecules on silica surface, Adv. Colloid Interface Sci., 121 (2006) 77–110.
[25] L.S. Oliveira, A.S. Franca, T.M. Alves, S.D.F. Rocha, Evaluation of untreated coffee husks as potential biosorbents for treatment of dye contaminated waters, J. Hazard. Mater., 155 (2008) 507–512.
[26] V. Vadivelan, K.V. Kumar, Equilibrium, kinetics, mechanism, and process design for the sorption of methylene blue onto rice husk, J. Colloid Interface Sci., 286 (2005) 90–100.
[27] Y. Bulut, H. Aydin, Kinetics and thermodynamics study of methylene blue adsorption on wheat shells, Desalination, 194 (2006) 259–267.
[28] R. Gong, M. Li, C. Yang, Y. Sun, J. Chen, Removal of cationic dyes from aqueous solution by adsorption on peanut hull, J. Hazard. Mater., 121 (2005) 247–250.
[29] G. Annadurai, R.-S. Juang, D.-J Lee, Use of cellulose based wastes for adsorption of dyes from aqueous solutions, J. Hazard. Mater., 92 (2002) 263–274.
[30] Z. Wang, P. Han, Y. Jiao, D. Ma, C. Dou, R. Han, Adsorption of congo red using ethylenediamine modified wheat straw, Desal. Water Treat., 30 (2011) 195–206.
[31] E. Bezak-Mazur, D. Adamczyk, Dyes adsorption on fresh and regenerated active carbon WD-extra, Rocz. Ochr. Sr., 13 (2011) 951–971.
[32] Y.S. Ho, G. Mckay, Pseudo-second order model for sorption processes, Process Biochem., 34 (1999) 451–465.
[33] S. Liu, Y. Ding, P. Li, K. Diao, X. Tan, F. Lei, Y. Zhan, Q. Li, B. Huang, Z. Huang, Adsorption of the anionic dye Congo red from aqueous solution onto natural zeolites modified with N,N-dimethyl dehydroabietylamine oxide, Chem. Eng. J., 248 (2014) 135–144.
[34] Y. Feng, H. Zhou, G. Liu, J. Qiao, J. Wang, H. Lu, L. Yang, Y. Wu, Methylene blue adsorption onto swede rape straw (Brassica napus L.) modified by tartaric acid: equilibrium, kinetic and adsorption mechanisms, Bioresour. Technol., 125 (2012) 138–144.
[35] S. Rangabhashiyam, N. Anu, M.S.G. Nandagopal, N. Selvaraju, Relevance of isotherm models in biosorption of pollutants by agricultural byproducts, J. Environ. Chem. Eng., 2 (2014) 398–414.
[36] A. Mittal, D. Jhare, J. Mittal, Adsorption of hazardous dye Eosin Yellow from aqueous solution onto waste material De-oiled Soya: Isotherm, kinetics and bulk removal, J. Mol. Liq., 179 (2013) 133–140.